THE JOURNAL OF BIOLOGICAL CHEMISTRY
Vol. 279, No. 42, Issue of October 15, pp. 43716–43724, 2004

Characterization of Acid-sensing Ion Channels in Dorsal Horn Neurons of Rat Spinal Cord*[S]

Received for publication, March 31, 2004, and in revised form, August 2, 2004
Published, JBC Papers in Press, August 9, 2004, DOI 10.1074/jbc.M403557200

Long-Jun Wu‡§, Bo Duan‡§, Yi-De Mei§, Jun Gao‡§, Jian-Guo Chen¶, Min Zhuo‖, Lin Xu, Mian Wu§, and Tian-Le Xu‡§‡‡**

*From the ‡Institute of Neuroscience, Shanghai Institutes for Biological Sciences, Chinese Academy of Sciences, Shanghai 200031, §School of Life Sciences, University of Science and Technology of China, Hefei 230027, ¶Department of Pharmacology, Tongji Medical College, Huazhong University of Science and Technology, Wuhan 430030, China, ‖Department of Physiology, University of Toronto, Toronto, Ontario M5S 1A1, Canada, and **Laboratory of Learning and Memory, Kunming Institute of Zoology, Chinese Academy of Sciences, Kunming 650223, China*

Acid-sensing ion channels (ASICs) are ligand-gated cation channels activated by extracellular protons. In periphery, they contribute to sensory transmission, including that of nociception and pain. Here we characterized ASIC-like currents in dorsal horn neurons of the rat spinal cord and their functional modulation in pathological conditions. Reverse transcriptase-nested PCR and Western blotting showed that three ASIC isoforms, ASIC1a, ASIC2a, and ASIC2b, are expressed at a high level in dorsal horn neurons. Electrophysiological and pharmacological properties of the proton-gated currents suggest that homomeric ASIC1a and/or heteromeric ASIC1a + 2b channels are responsible for the proton-induced currents in the majority of dorsal horn neurons. Acidification-induced action potentials in these neurons were compatible in a pH-dependent manner with the pH dependence of ASIC-like current. Furthermore, peripheral complete Freund's adjuvant-induced inflammation resulted in increased expression of both ASIC1a and ASIC2a in dorsal horn. These results support the idea that the ASICs of dorsal horn neurons participate in central sensory transmission/modulation under physiological conditions and may play important roles in inflammation-related persistent pain.

Tissue acidosis, associated with inflammation, ischemia/hypoxia, and tumorigenesis, contributes to pain sensation and hyperalgesia (1). Recent studies demonstrate that the dorsal root ganglion (DRG)[1] neurons and neurons in the central nervous system directly respond to a reduction in external pH via the vanilloid receptor (VR1) (2) and the acid-sensing ion channels (ASICs) (3, 4). Four genes and six major transcripts coding for ASICs have been identified (5–12). Both homomers of ASIC1a, ASIC1b, ASIC2a, and ASIC3 and heteromers of ASIC1a + 2a, ASIC2a + 2b, ASIC1a + 3, ASIC2a + 3, and ASIC2b + 3 can form functional channels, each having distinct electrophysiological and pharmacological characteristics (3, 4).

ASICs have been suggested to play important roles in physiological/pathological conditions, from sensory transmission (such as touch, taste, and nociception) (13–17) to behavioral memory, retinal function, seizure, and ischemia (18–22). In particular, increased expression of ASIC1a, ASIC2b, and ASIC3 in the DRG was detected after peripheral inflammation (23). The increased ASIC expression may contribute to the enhanced excitability of the DRG neuron after inflammation (24). The roles of ASICs in nociception, however, are not limited to the DRG cells (25). The dorsal horn of spinal cord, the first central site for integration, relay, and modulation of nociceptive information, is an important area to investigate. For example, transcripts of ASICs have been localized to the spinal cord (10, 26), and acid-activated currents have been detected in cultured spinal ventral horn neurons (27). However, less is known about the molecular identity and functional roles of ASICs in spinal dorsal horn neurons.

In the present study, we have investigated the functional and biochemical properties of ASICs in dorsal horn neurons of the rat spinal cord by using conventional whole-cell patch clamp electrophysiology, reverse transcriptase (RT)-nested PCR, and Western blotting techniques. Comparison of the properties with those of cloned ASIC channels suggests that homomeric ASIC1a and/or heteromeric ASIC1a + 2b channels are responsible for the proton-induced currents in the majority of dorsal horn neurons. Acidification-induced action potentials in these neurons, as well as the increased expression of the spinal ASICs by periphery inflammation, suggests the physiological involvement of ASICs in central pain sensing under physiological and/or pathological conditions.

MATERIALS AND METHODS

Isolation of Neurons—The experimental protocols were approved by our Institutional Care and Use of Animals Committee. The dorsal horn neurons were mechanically dissociated from rat spinal cord as described previously (28). In brief, 2-week-old Wistar rats were sacrificed by decapitation, and a segment of lumbosacral (L4-S2) spinal cord was dissected out. Thereafter, transverse slices at 400 μM were sectioned with a vibratome tissue slicer (VT1000S, Leica instruments, Ltd., Wetzlar, Germany) in the incubation solution (see "Solutions and Drugs" for the composition). A vibration-isolation system (29) was then used to mechanically dissociate dorsal horn neurons from the slices. Briefly, a fire-polished glass pipette mounted on a vibrator touched lightly and vibrated horizontally at about 5–10 Hz on the surface of the slices under the control of a

* This study was supported by the National Basic Research Program of China (G1999054000), the National Natural Science Foundation of China (30125015, 30321002, 30170247, 30228020), and the Knowledge Innovation Project from the Chinese Academy of Sciences (KSCX 2-SW-217, KSCX 2-2-04) (to T.-L. X.) The costs of publication of this article were defrayed in part by the payment of page charges. This article must therefore be hereby marked "*advertisement*" in accordance with 18 U.S.C. Section 1734 solely to indicate this fact.

[S] The on-line version of this article (available at http://www.jbc.org) contains a supplemental figure.

‡‡ To whom correspondence should be addressed: Institute of Neuroscience, Shanghai Institutes for Biological Sciences, Chinese Academy of Sciences, 320 Yue-yang Road, Shanghai 200031, China. Tel.: 86-21-5492-1751; Fax: 86-21-5492-1735; E-mail: tlxu@ion.ac.cn.

[1] The abbreviations used are: DRG, dorsal root ganglion; ASIC, acid-sensing ion channel; CFA, complete Freund's adjuvant; RT, reverse transcriptase; MES, 2-(*N*-morpholino)ethanesulfonic acid; NMDG, *N*-methyl-D-glucamine; ANOVA, analysis of variance; NMDA *N*-methyl-D-aspartate.

pulse generator. The vibration-dissociation lasted for about 10 min, and then the slices were removed from the dish. Within 20 min after dissociation, isolated dorsal horn neurons attached to the bottom of the culture dish and the fusiform cells with oval or triangular soma (15–25 μm in diameter) were selected for electrophysiological experiments.

Cell Culture and Transfection—All constructs were expressed in HEK293T cells. HEK293T cells were cultured at 37 °C in a humidified atmosphere of 5% CO_2 and 95% air. The cells were maintained in Dulbecco's modified Eagle's medium (Invitrogen) supplemented with 2 mM L-glutamine, 10% fetal bovine serum, and 100 units/ml penicillin/streptomycin. Transient transfection of HEK293T cells was carried out using the conventional calcium phosphate method. Co-transfection with a green fluorescent protein expression vector, pEGFP, was used to enable identification of transfected cells for patch clamping by monitoring its fluorescence. When more than one of the ASIC subunits were expressed, the multiplasmids were co-tranfected in a 1:1 ratio. Electrophysiological measurements were performed 16–48 h after transfection. GW1-CMV-ASIC1a and GW1-CMV-ASIC2a were generous gifts from Dr. Jun Xia (The Hong Kong University of Science and Technology, Hong Kong, China). pN1z-ASIC2b was kindly provided by Dr. Philip K. Ahring (NeuroSearch A/S, Ballerup, Denmark). pEGFP was from Dr. Jian-hong Luo (Zhejiang University Faculty of Medicine, Hangzhou, China).

Solutions and Drugs—The ionic composition of the incubation solution was (mM): 124 NaCl, 24 $NaHCO_3$, 5 KCl, 1.2 KH_2PO_4, 2.4 $CaCl_2$, 1.3 $MgSO_4$, and 10 glucose, aerated with 95% O_2/5% CO_2 to a final pH of 7.4. The standard external solution contained (mM): 150 NaCl, 5 KCl, 1 $MgCl_2$, 2 $CaCl_2$, and 10 glucose, buffered to various pH values with either 10 mM HEPES, pH 6.0–7.4, or 10 mM MES, pH <6.0. In Na^+-free medium, Na^+ was substituted with equimolar NMDG, and in Ca^{2+}-free medium, Ca^{2+} was substituted with 5 mM EGTA. The glucose-free solution was prepared by replacing glucose with equimolar mannitol. The patch pipette solution for whole-cell patch recording was (mM): 120 KCl, 30 NaCl, 1 $MgCl_2$, 0.5 $CaCl_2$, 5 EGTA, 2 Mg-ATP, 10 HEPES. The internal solution was adjusted to pH 7.2 with Tris base. When the current-voltage relationships for proton-induced currents were examined, 300 nM tetrodotoxin and 200 μM $CdCl_2$ were added to the standard external solution, and K^+ was substituted with Cs^+ in the internal solution.

For measurement of the permeability of monovalent cations, the internal solution contained (mM) 160 NaCl, 10 EGTA, and 10 HEPES, and the external solution contained (mM) 160 test cation (*X*), 10 HEPES, and 12 glucose. The relative permeability of Cs^+ and K^+ was measured by comparing the reversal potentials when electrodes contained CsCl, KCl, or NaCl with extracellular NaCl in each case. Because of the inhibition of proton-induced currents by external Ca^{2+}, Ca^{2+} permeability was measured under low Ca^{2+} external solution containing (mM) 5 $CaCl_2$, 150 NMDG, 10 HEPES, and 12 glucose, and the internal solution contained (mM) 160 NaCl, 5 EGTA, and 10 HEPES. The osmolarity and pH of all these solutions were maintained at 300–325 milliosmole/liter (Advanced Instrument, Norwood, MA) and 7.2–7.4, respectively.

All drugs were from Sigma (St. Louis, MO). Drugs were applied using a rapid application technique termed the "Y-tube" method throughout the experiments (28). This system allows a complete exchange of external solution surrounding a neuron within 20 ms.

Electrophysiology—The electrophysiological recordings were performed in the conventional whole-cell patch recording configuration under voltage clamp or current clamp conditions. Patch pipettes were pulled from glass capillaries with an outer diameter of 1.5 mm on a two-stage puller (PP-830, Narishige Co., Ltd., Tokyo, Japan). The resistance between the recording electrode filled with pipette solution and the reference electrode was 4–6 MΩ. Membrane currents or potentials were measured using a patch clamp amplifier (Axon 200B, Axon Instruments, Foster City, CA) and were sampled and analyzed using a Digidata 1320A interface and a computer with the Clampex and Clampfit software (version 8.0.1, Axon Instruments). In most experiments, 70–90% series resistance was compensated. Unless otherwise noted, the membrane potential was held at −50 mV throughout the experiment, under voltage clamp conditions. All the experiments were carried out at room temperature (22–25 °C).

Inflammation Experiments—Right hindpaws of anesthetized Wistar rats (4–5 weeks old) were inflamed by an injection of 100 μl of complete Freund's adjuvant (CFA) (50%). Both hindpaws were tested individually for withdrawal latency by measuring the response to the radiant heat stimulus. In brief, the inflamed animals were placed in individual plexiglass cages and allowed to acclimate to the testing environment for 30 min. Thereafter, radiant heat was turned on and focused on a small region of their hindpaws. When the animals withdrew their paws, stimulation ended. Both treated and untreated paws were tested so that each animal was its own control. The interval between tests of the same paw was at least 5 min. The average of five tests on each paw at each time point represented the withdrawal latency. L4–L5 spinal cords were removed at 1 h, 1 day, and 3 days after injection. The removed spinal cord was divided laterally into an ipsi- and contralateral half. The latter one was used as the negative control. Vehicle-injected rats were used as controls.

RT-PCR Experiments—The sequences of primers used in this study are listed as follows: P1, 5′-ATGGAATTGAAGACCGAGGAGGAG-3′; P2, 5′-CGCTGCAGGCCTCCCCACGGAAGT-3′; P3, 5′-ATGGACCTCAAGGAGAGCCCCAGT-3′; P4, 5′-GATGCCCACACTCCTGCCCCTTGA-3′; P5, 5′-ACCGCGCTCAGCGGC-3′; P6, 5′-GCGGCAGGAAGAGGC-3′; P7, 5′-ATGCCCATCCAGATCTTTTGTTCT-3′; P8, 5′-AGAAAGCCTCTGGGCCAGGAGGAG-3′; P9, 5′-ATGAAACCTCGCTCCGGACTGGAG-3′; P10, 5′-GATCACTGTGAAGTTCTCAGGCCC-3′; P11, 5′-GAGGAGGAGGAGGTGGGTGGTGTC-3′; P12, 5′-CACGGAAGTGGCACGAGAGCAGCA-3′; P13, 5′-AGCCCCAGTGAGGGCAGCCTGCAA-3′; P14, 5′-GCCCCTTGAACTTGCAGTAGAGCA-3′; P15, 5′-ACCGCGCTCAGCGGC-3′; P16, 5′-GCGGCTCGTCGCCCCGCA-3′.

Total RNA of spinal cord was extracted using an RNA extraction kit (Promega). One μg of total RNA was used as a template for cDNA synthesis and subsequent amplification with the One Step RNA PCR kit (Takara Shuzo, Kyoto, Japan). Primer pairs P1/P2, P3/P4, P5/P6, P7/P8, and P9/P10 were used for amplification of the transcripts of ASIC1a, ASIC2a, ASIC2b, ASIC1b, and ASIC3, respectively. To confirm the transcription of ASICs in dorsal horn neurons, the RT-nested PCR method was applied to amplify ASIC1a, ASIC2a, and ASIC2b, which are implicated to be expressed mainly in the central nervous system (4). In brief, 20–30 acutely isolated dorsal horn neurons were suctioned into a suction pipette (the tip diameter is 30–50 μm). Thereafter, the neurons were lysed, and the lysate was then used as a template for the RT-nested PCR. The primary RT-PCR was the same as described under "RT-PCR Experiments." A nested secondary PCR amplification was then performed to amplify the smaller ASIC1a, ASIC2a,and ASIC2b fragments, using the primers of P11/P12, P13/P14, and P15/P16 respectively.

PCR products were analyzed on 1% agarose gels by ethidium bromide staining. The purified PCR products were then subcloned into pGEM-T vector. DNA sequence verification was performed using the ABI Prism (Applied Biosystems, Foster City, CA), automated sequencing method.

Western Blotting—Spinal cord was lysed in lysis buffer (150 mmol/liter Nacl, 1.0% Nonidet P-40, 0.5% deoxycholate, 0.1% SDS, 50 mmol/liter Tris, pH 8.0) supplemented with protease inhibitor mixture (Roche Applied Science). Protein concentration was determined by the BCA-200 protein assay kit (Pierce). The lysates (20 μg) were resolved by denaturing 12% SDS-PAGE and then transferred to nitrocellulose membranes. The membranes were probed with primary affinity-purified rabbit polyclonal antibody against ASIC1a, ASIC2a, and ASIC2b (Alpha Diagnostic International, San Antonio, TX) followed by secondary goat anti-rabbit alkaline phosphatase-conjugated antibody (Promega). The blots were then developed with the Western Blue® stabilized substrate for alkaline phosphatase.

Data Analysis—Results were expressed as the mean ± S.E. Statistical comparisons were made with the Student's *t* test. Analysis of variance (ANOVA) for multiple comparisons was used as noted. In all cases, $p < 0.05$ (*) or 0.01 (**) was considered significant as shown in Figs. 2, 6, and 7. The permeability ratio of P_X/P_{Na} was calculated from the modified Goldmann-Hodgkin-Katz equation: $P_X/P_{Na} = \exp(\Delta V_{rev}F/RT)$ due to the equimolar cations in external and internal solution, where ΔV_{rev} is the change in reversal potential when Na^+ was replaced by the tested cation, F is the Faraday constant, R is the gas constant, and T is the absolute temperature. P_{Na}/P_{Ca} was calculated from: $P_{Na}/P_{Ca} = [Na^+]_i \exp(V_{rev}F/RT)(1 + \exp(V_{rev}F/RT))/4[Ca^{2+}]_o$. We consider the effect of NMDG negligible in the equation, as it is nearly impermeable to ASICs.

RESULTS

Electrophysiologial Recordings of ASIC-like Current from Spinal Cord Dorsal Horn Neurons—ASIC-like currents were found in DRG cells as well as in central neurons (30, 31); however, no studies have been reported on spinal dorsal horn neurons. To investigate the ASIC-like currents in acutely dissociated spinal dorsal horn neurons, whole-cell patch clamp recordings were used, and acidic pH-buffered solution was applied. At a holding potential (V_H) of −50 mV, fast reduction of

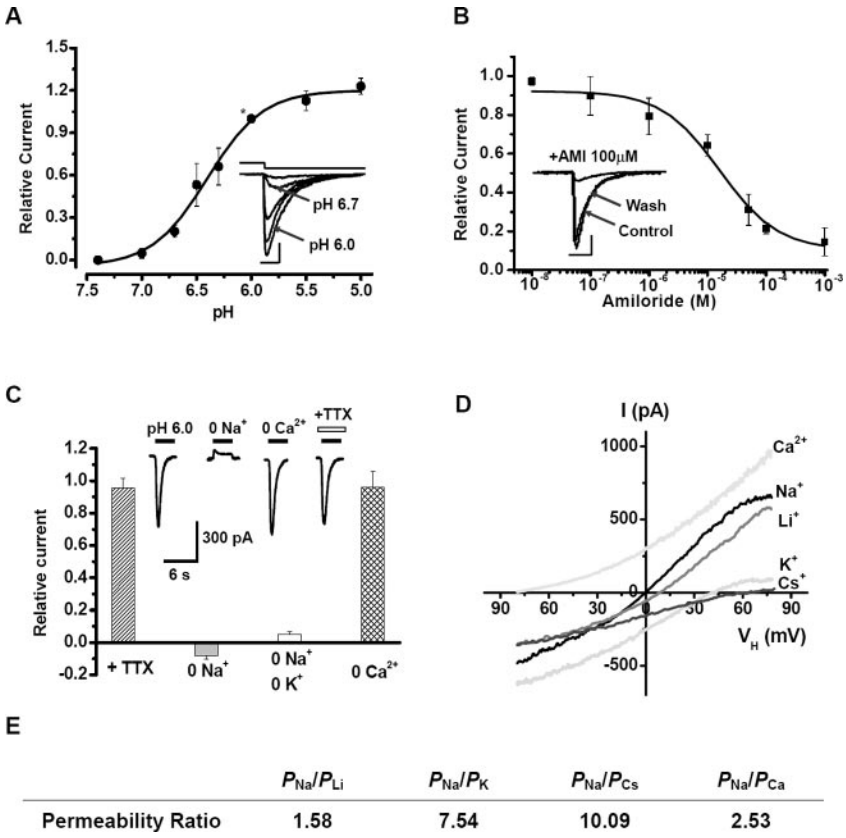

FIG. 1. **Electrophysiological characterizations of proton-induced currents in dorsal horn neurons of rat spinal cord.** *A*, pH dependence of the proton-induced currents. *B*, pH (6.0)-evoked transient current was inhibited reversibly and dose dependently by amiloride (*AMI*). The *scale bar* is 200 pA/1 s. All currents were normalized to the peak response induced by pH 6.0 (*). *C*, inward current of similar amplitude could be triggered in the presence of 300 nM tetrodotoxin (*TTX*) or Ca^{2+}-free medium, whereas in Na^+-free saline, the inward current was virtually undetectable. *D*, current (*I*)-voltage (*V*) relationships of the proton-induced currents obtained by the voltage ramp protocol (from −80 to +80 mV in 700 ms) in 5 mM Ca^{2+} external solution, Na^+-rich external solution, Li^+-rich external solution, K^+-rich internal solution, or Cs^+-rich internal solution. *E*, permeability ratios of P_{Na}/P_{Li}, P_{Na}/P_K, P_{Na}/P_{Cs}, and P_{Na}/P_{Ca} were further determined. In this and subsequent figures, the *horizontal bars* above each current trace indicate the application of the extracellular pH or drugs. Each point or column represents the average of six to eight neurons, and the *vertical bars* show the mean ± S.E. Holding potential (V_H) was −50 mV.

extracellular pH evoked rapidly desensitizing inward currents with an average decay time constant of 1.18 ± 0.37 s in most neurons (181/200), the amplitude of which increased with decreasing extracellular pH, with the threshold around pH 7.0–6.8 and a half-maximum activation (pH_{50}) value of pH 6.38 (Fig. 1*A*). The average amplitude of pH 6.0-induced currents was 420.5 ± 63.6 pA (n = 15). The currents could be reversibly inhibited by amiloride, a selective antagonist for cloned ASICs (7), in a dose-dependent manner, with the half-maximal inhibition (IC_{50}) value of 16.2 μM (Fig. 1*B*). Interestingly, in a minority of neurons (19/200), the pH 6.0 solution evoked responses with much longer duration (decay time of 4.52 ± 0.69 s, data not shown). Because of the low incidence, we did not include this minority in the present study. Therefore, we only focused on the rapidly decaying proton-evoked current in the following assays.

The reversal potential of the currents, estimated from the current-voltage relationships, was 35.3 ± 2.8 mV (n = 11), which is close to the theoretical Na^+ equilibrium potential (41.2 mV) calculated with the Nernst equation for the given extra- and intracellular Na^+ concentrations (150 and 30 mM, respectively). When the extracellular Na^+ was substituted by NMDG, the amplitude of the current was remarkably inhibited (Fig. 1*C*). These results suggest that the proton-induced currents are mainly due to an increase of the Na^+ conductance. For quantitative estimation of the permeability of the proton-gated channel for cations, a voltage ramp protocol was applied under bi-ionic conditions (Fig. 1*D*). When equimolar Na^+ was present in both the intracellular and extracellular solutions, the proton-induced currents exhibited a reversal potential close to 0 mV (−2.0 ± 1.1 mV, n = 5) as expected. Substitution of extracellular Na^+ with Li^+ shifted the reversal potential to 9.4 ± 0.9 mV (n = 5), and substitution of intracellular Na^+ with K^+ or Cs^+ shifted the reversal potential to 48.9 ± 6.3 mV (n = 7) and 56.2 ± 9.8 mV (n = 5), respectively. The reversal potential moved to −73.4 ± 2.5 mV (n = 6) when low Ca^{2+} external solution was applied. Relative permeability ratios were then calculated (Fig. 1*E*) according to the method described under "Materials and Methods." These results indicate that the channel underlying the proton-induced currents in rat dorsal horn neurons is permeable to Na^+, Li^+, Ca^{2+}, K^+, and Cs^+ with a permeability preference of $P_{Na} > P_{Li} > P_{Ca} > P_K > P_{Cs}$.

Different ASIC subunits have different sensitivity to extracellular Ca^{2+} and Zn^{2+} ($[Ca^{2+}]_o$ and $[Zn^{2+}]_o$) (7, 32, 33). Thus, we tested the effects of Ca^{2+} and Zn^{2+} on the proton-induced currents, which would help us identify the subunit composition of ASICs underlying the current in dorsal horn neurons. As shown in Fig. 2*A*, pH (6.0)-gated current was inhibited by high $[Ca^{2+}]_o$ and was almost eliminated in 20 mM $[Ca^{2+}]_o$. The IC_{50} of $[Ca^{2+}]_o$ inhibition was 4.1 mM. The underlying mechanisms of Ca^{2+} modulation of ASICs have been proposed to be an extracellular effect by several groups (33, 34). However, considering the relatively high Ca^{2+} permeability for the native channel in the present preparation, it is possible that the effects of extracellular Ca^{2+} are because of the feedback inhibition by Ca^{2+} influx. To study this possibility, intracellular pipette solution with high Ca^{2+} was used. However, we did not observe any inhibition of proton-induced current by intracellular high Ca^{2+} (see Supplement 1).

The modulation of $[Zn^{2+}]_o$ was then studied. As shown in Fig. 2*B*, $[Zn^{2+}]_o$ exerted no significant inhibition on the peak amplitude of the currents. Interestingly, $[Zn^{2+}]_o$ produced a biphasic modulatory effect on the decay time constant (τ) of the currents (Fig. 2*B*). In particular, the averaged τ was decreased by 1 μM $[Zn^{2+}]_o$ to 77.2 ± 3.8% ($p < 0.05$, n = 8), and increased by 1 mM $[Zn^{2+}]_o$ to 182.2 ± 12.7% ($p < 0.01$, n = 8) of the control value activated by pH 6.0.

RT-PCR and Biochemical Study of ASICs in Dorsal Horn Neurons—Next, we performed RT-PCR to examine the molecular identity of ASICs in the dorsal horn of rat spinal cord. We did not consider ASIC4 in the present study, because it was

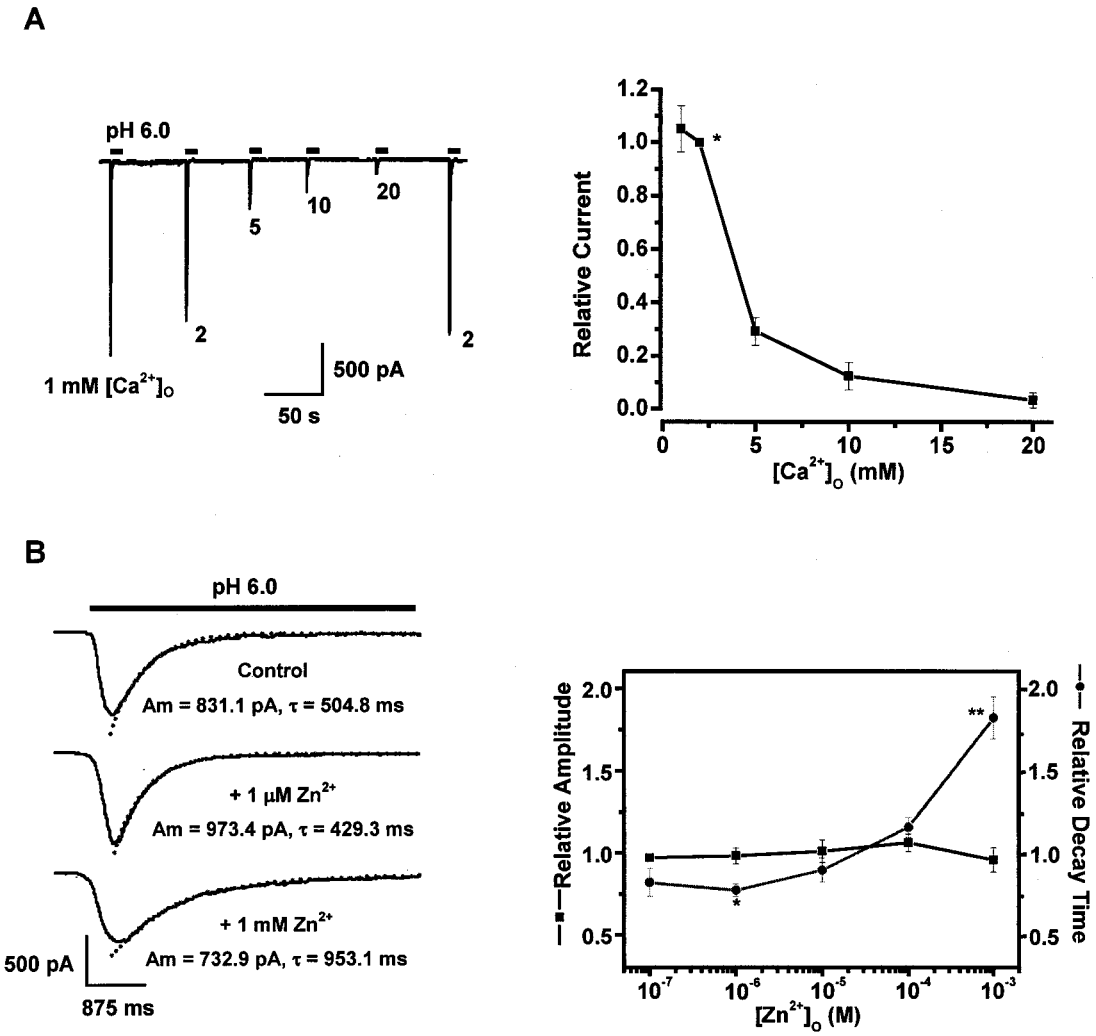

FIG. 2. **Modulation of the proton-induced currents by extracellular Ca^{2+} ($[Ca^{2+}]_o$) and Zn^{2+} ($[Zn^{2+}]_o$).** *A*, $[Ca^{2+}]_o$ inhibited the proton-induced currents. All currents were normalized to the peak response of proton-induced currents recorded at 2 mM $[Ca^{2+}]_o$ (*). *B*, modulatory effect of $[Zn^{2+}]_o$ on the proton-induced currents. The decay time constant (τ) of the current induced by pH 6.0 decreased by 1 μM $[Zn^{2+}]_o$ but increased by 1 mM $[Zn^{2+}]_o$, whereas the peak amplitude (*Am*) of the current (normalized to the control response of pH 6.0) was unaffected by either 1 μM or 1 mM $[Zn^{2+}]_o$. The decay of the proton-induced currents was well fitted using a single exponential equation (*dotted lines*). *, $p < 0.05$, **, $p < 0.01$ (Student's paired *t* test).

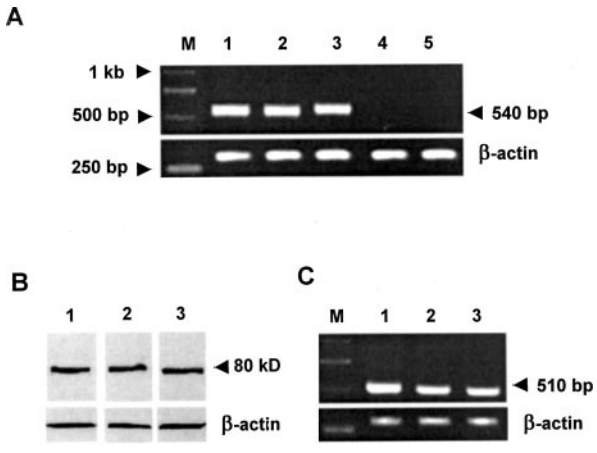

FIG. 3. **Expression of ASICs in dorsal horn neurons.** *A*, ASIC1a, ASIC2a, and ASIC2b transcripts were detected, whereas ASIC1b and ASIC3 were undetectable in the dorsal horn of the spinal cord using RT-PCR. *B*, ASIC1a, ASIC2a, and ASIC2b proteins were detected in the dorsal horn using Western blotting. *C*, The RT-nested PCR was used to assess ASIC1a, ASIC2a, and ASIC2b expression in a total of 20–30 acutely dissociated dorsal horn neurons. β-actin was used as an internal control. *M*, marker; *lanes 1–5,* ASIC1a, ASIC2a, ASIC2b, ASIC1b, and ASIC3, respectively.

found unresponsive to a drop in pH in either homomeric or heteromeric form (11, 12). As shown in Fig. 3*A*, ASIC1a, ASIC2a, and ASIC2b were prominent isoforms, whereas ASIC1b and ASIC3 were not detected in the dorsal horn. Further DNA sequencing of the PCR products confirmed their identity as the expected portions of the corresponding genes. Consistent with this result, our Western blotting analysis showed that ASIC1a, ASIC2a, and ASIC2b proteins were expressed at high level in the dorsal horn (Fig. 3*B*). To verify directly the ASIC expression in individual dorsal horn neurons, we performed RT-nested PCR using 20–30 isolated neurons. Abundant expression of the ASIC1a, ASIC2a, and ASIC2b transcripts were detected in these neurons (Fig. 3*C*). The ratios of band intensity (normalized to β-actin) of ASIC1a to ASIC2a and ASIC2b in Fig. 3 are 1.83 and 1.67, respectively.

The expression of ASIC1a, ASIC2a, and ASIC2b suggests that the possible ASIC channels responsible for the proton-induced currents are homomeric ASIC1a, ASIC2a, or heteromeric ASIC1a + 2a, ASIC2a + 2b, ASIC1a + 2b, ASIC1a + 2a + 2b. All these cloned channels have been well studied in an *in vitro* expression system, except ASIC1a + 2b and ASIC1a + 2a + 2b (7, 9, 35, 36). Table I summarizes the properties of the proton-gated currents detected in the present preparation and those of

TABLE I
Functional properties of the proton-activated current in dorsal horn neurons
Numbers in the parentheses represent the cited literature.

Properties	Present preparation	ASIC1a (7)	ASIC2a (36)	ASIC1a + 2a (35)	ASIC2a + 2b (9)
τ_{des} [a]	1.18 ± 0.37 s	~1.40 s	1.65 ± 0.20 s	~2.20 s	~3.50 s
I_{sus}/I_{peak} (%)	0.97 ± 0.19	2.5 ± 1.5 (41)	7.5 ± 0.8 (41)	5.7 ± 1.7 (41)	17 ± 1.6 (41)
$pH_{threshold}$	7.0 ~ 6.8	6.9	5.0	6.2	6.5
pH_{50}	6.38	6.1	4.35	4.8	4.0
Ion selectivity	$Na^+ > Li^+ > Ca^{2+} > K^+ > Cs^+$	$Na^+ > Ca^{2+}K^+$	$Na^+ >> K^+$	$Na^+ > K^+ > Ca^{2+}$	Na^+ (transient); Na^+, K^+ (sustained)
Amiloride IC_{50}	16.2 μM	10 μM	28 μM	20 μM	Completely blocked by 500 μM amiloride
$[Ca^{2+}]_o$ IC_{50}	4.1 mM	3 ~ 5 mM	>10 mM(33)	>10 mM (33)	—[b]
$[Zn^{2-}]_o$ EC_{50}	No effect on the amplitude	No effect on the amplitude (32)	120 μM (32)	111 μM (32)	—[b]

[a] τ_{des}, desensitization time constant.
[b] —, present unknown data.

homomeric ASIC1a or ASIC2a and heteromeric ASIC1a + 2a or ASIC2a + 2b, showing that the present current phenotype (but not the other three) was best matched to homomeric ASIC1a-mediated current. To further assess the possible involvement of ASIC1a + 2b and ASIC1a + 2a + 2b, we studied ASICs transfected in HEK293T cells. Desensitization time constant (τ_{des}) and the ratio of sustained current and peak current (I_{sus}/I_{peak}) were tested (Fig. 4). The τ_{des} of ASIC1a + 2a + 2b channel was significantly slower than that of native channel in dorsal horn neurons (2.00 ± 0.11 *versus* 1.18 ± 0.37, $n = 6–8$, $p < 0.001$). However, the values for τ_{des} of ASIC1a and ASIC1a + 2b were not significantly different from that of the native channel. A sustained current was evident for ASIC1a + 2a + 2b (I_{sus}/I_{peak} = 18.87 ± 0.73%, $n = 5$) but subtle for ASIC1a + 2b (I_{sus}/I_{peak} = 2.75 ± 0.47%, $n = 6$), ASIC1a (I_{sus}/I_{peak} = 0.43 ± 0.04%, $n = 6$), and the native channel (I_{sus}/I_{peak} = 0.80 ± 0.97%, $n = 8$).

Effect of ASIC-like Current on the Excitability of Dorsal Horn Neurons—Synaptic vesicle contents are acidic (pH 5.6), and a transient drop in extracellular pH is associated with synaptic transmission (37). We next tested whether endogenous ASICs contribute to physiological functions of dorsal horn neurons in hippocampal neurons as reported previously (31). Membrane potential variation was examined under the current clamp condition when acidic stimulations were applied to dorsal horn neurons. The resting potential of the dissociated neurons was −52.5 ± 3.8 mV ($n = 15$). Typical changes of membrane potential elicited by shifting pH from 7.4 to 6.6, 6.3, and 6.0 were shown in Fig. 5*A*. Activation of ASIC-like current by pH 6.6 transiently depolarized the neurons, and pH 6.3 induced more depolarization, which accompanied the appearance of a single action potential. When pH 6.0 external solution was applied, the neuron was depolarized to ~0 mV with a train of action potentials at the initial transient depolarization. The pH dependence of the action potential triggering is compatible with the pH dependence of ASIC-like current (Fig. 1*A*). The depolarization was highly attenuated by the ASIC inhibitor amiloride (100 μM). Blocking voltage-gated Na^+ channel with tetrodotoxin (300 nM), however, had little effect on the depolarization but completely diminished the action potentials induced by the low pH solution (Fig. 5*B*). These results indicate that activation of ASIC-like current increases the excitability of dorsal horn neurons.

Inflammation Increases the Expression of Spinal ASICs—Inflammation increases the activity of peripheral nerves, facilitating the synaptic transmission to dorsal horn neurons. Furthermore, inflammation is associated with activity-dependent long term changes in the spinal cord (38). In DRG neurons, increased expressions of ASIC subunits have been reported in inflammatory pain (23). Thus, we were stimulated to study the spinal expression of ASIC subunits following chronic CFA-induced inflammation. A subcutaneous injection of CFA into the hindpaw resulted in an obvious inflammatory response as evident by swelling and redness of the entire paw shortly after injection. Fig. 6*A* shows changes in the paw withdrawal latency in CFA-treated paws. Compared with that of CFA-untreated paws, paw withdrawal latency of treated paws was significantly reduced at 1 h and lasted the following test time points (1 and 3 days post-injection). ASIC expression levels were examined by Western blotting analysis made from control (vehicle injected), contralateral (uninflamed), and ipsilateral (inflamed) spinal cord at 1 h, 1 day, and 3 days. As shown in Fig. 6, *B* and *C*, there was a significant increase in intensity of ASIC1a and ASIC2a proteins in ipsilateral compared with contralateral cords or control groups in 1 and 3 days after inflammation. No significant difference was observed for ASIC1a and ASIC2a expression between contralateral cord and control. The expression of ASIC2b showed no significant increase in both ipsilateral and contralateral cords compared with control. Semi-quantitative RT-PCR was then used to confirm the results. Consistent with the Western blotting results, RT-PCR analysis indicated that CFA-induced inflammation increased the mRNAs of both ASIC1a and ASIC2a in ipsilateral cords in 1 and 3 days after inflammation (Fig. 7, *A* and *B*).

DISCUSSION

Our results demonstrate that homomeric ASIC1a and/or heteromeric ASIC1a + 2b channels are responsible for the proton-induced currents in the majority of dorsal horn neurons. The identification of the channel subtypes on different populations of neurons is essential to understanding their functional implications and to develop pharmacological strategies able to interfere selectively with specific neuronal functions. More importantly, the up-regulation of ASIC1a and ASIC2a expression by peripheral inflammation suggests the physiological involvement of ASICs in central pain sensing under physiological and/or pathological conditions.

Identification of ASICs in Spinal Dorsal Horn Neurons—Using sensitive RT-PCR technique, we were unable to detect ASIC1b and ASIC3 transcripts in the rat spinal dorsal horn. This result is consistent with previous reports that ASIC1b and ASIC3 are exclusively expressed in sensory ganglia (8, 10). Thus, the existence of the homomers of ASIC1b and ASIC3, as well as the heteromers of ASIC1a + 3, ASIC2a + 3, and ASIC2b + 3, in rat dorsal horn neurons could be immediately excluded. Our electrophysiological data showed that the proton-induced currents in dorsal horn neurons inactivated rapidly with the decay time of 1.18 ± 0.37 s, was sensitive to amiloride (IC_{50} = 16.2 μM), and had a threshold of pH 7.0–6.8 with the pH_{50} of pH 6.38. The ion selectivity of the currents was

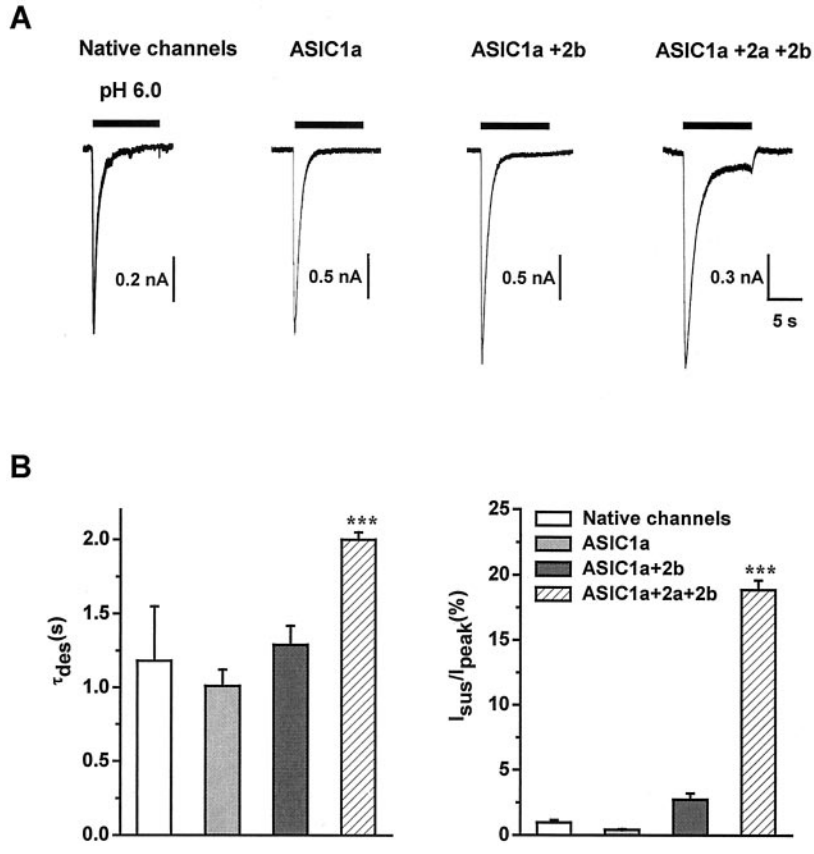

FIG. 4. **Both ASIC1a-and ASIC1a + 2b channel-mediated currents mimic the proton-induced current in spinal dorsal horn neurons.** *A*, typical traces for pH (6.0)-induced currents in dorsal horn neurons (native channel), HEK293T cells expressing ASIC1a, ASIC1a + 2b, and ASIC1a + 2a + 2b channels. *B*, statistical results showing the desensitization time constant (τ_{des}) and the I_{sus}/I_{peak} of the recordings shown in *A*. ***, $p < 0.001$ (Student's unpaired *t* test).

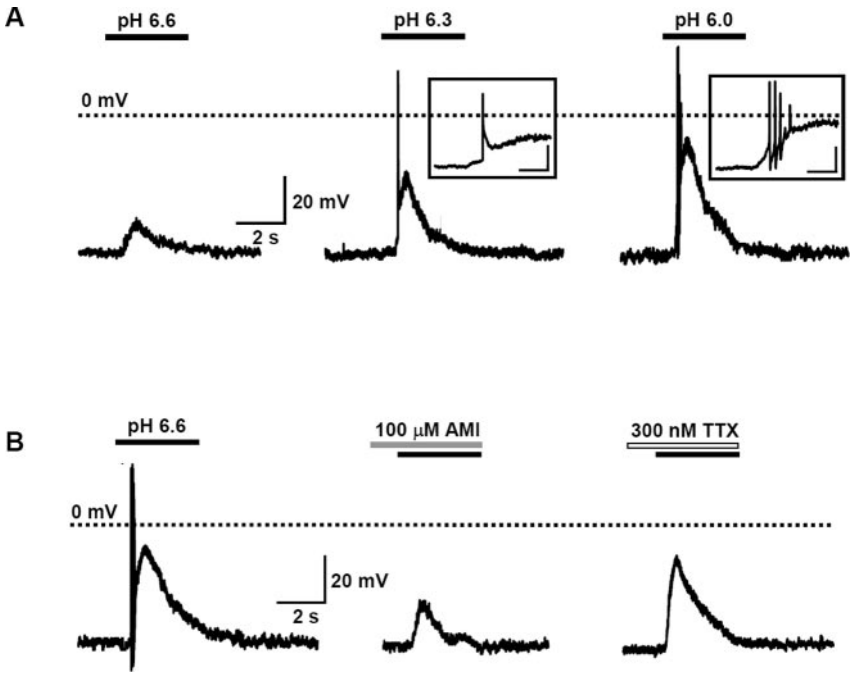

FIG. 5. **ASIC-like current regulates dorsal horn neuron excitability.** *A*, membrane depolarization was induced by applying pH 6.6, 6.3, and 6.0 in a dorsal horn neuron. *Inset*, the initial acid-induced depolarization and the subsequently triggered action potentials are shown on a larger scale. The *scale bar* is 25 mV/200 ms. *B*, amiloride (100 μM) decreased the depolarization by pH 6.0 application, and tetrodotoxin (300 nM) diminished the action potentials without affecting the depolarization. The membrane potential was recorded in current clamp mode with 0 pA current. *Dashed lines* indicate 0 mV.

$P_{Na} > P_{Li} > P_{Ca} > P_K > P_{Cs}$. The peak amplitude of the currents was inhibited by the extracellular Ca^{2+} but not by Zn^{2+}. All these results collectively point to homomeric ASIC1a mediating the proton-induced currents in the present preparation. The following evidence further supports this assumption. First, the present proton-induced currents (native channels) and *in vitro*-expressed homomeric ASIC1a have similar thresholds for opening at about pH 6.9 and are hypersensitive to extracellular proton (pH_{50} = ~6.1) (7), whereas the homomeric ASIC2a or heteromers of ASIC1a + 2a and ASIC2a + 2b channels are less sensitive to the drops in the extracellular pH (Table I) (9, 35, 36). Second, the ion selectivity of the currents in the present preparation is similar to that of cloned ASIC1a reported by Waldmann *et al.* (7) but differs from that of either ASIC2a homomers or heteromeric ASIC1a + 2a channels (Table I) (35, 36). Particularly, our data showed that native channels were Ca^{2+}-permeable (Fig. 1*E*). Consistent with this result, a recent report using Ca^{2+} imaging demonstrates that activation of neuronal ASIC1a (but not ASIC2a or ASIC1a + 2a) channels increases the cytosolic Ca^{2+} concentration, indicating the rel-

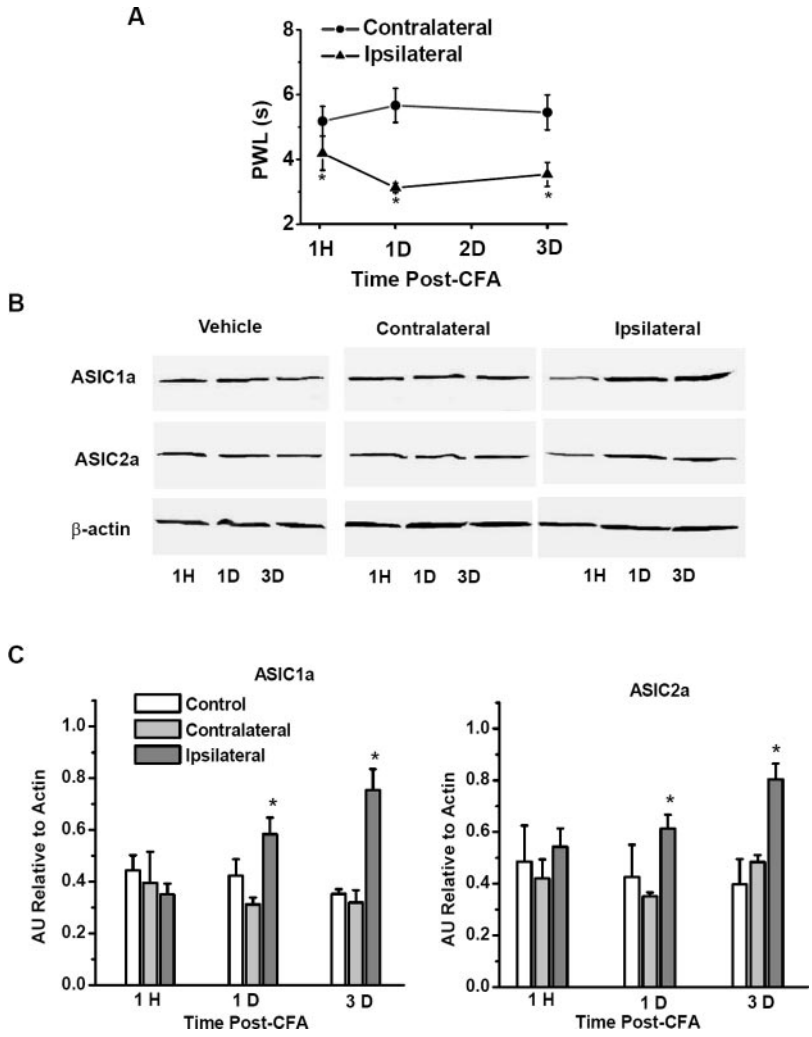

FIG. 6. **Up-regulation of dorsal horn ASIC1a and ASIC2a proteins by periphery inflammation.** *A*, changes in paw withdrawal latency (*PWL*) of the rat after CFA injection. PWL was measured in CFA-treated hindpaw (ipsilateral) and untreated (contralateral) hindpaws. *B*, representative experiments showing Western blotting results of ASIC1a and ASIC2a proteins in L4–L5 spinal cord from vehicle and CFA-treated rats. *C*, ipsilateral spinal cord showed a significant increase in band intensity (normalized to β-actin) of ASIC1a and ASIC2a proteins at day 1 and 3 compared with contralateral or vehicle control spinal cord. *, $p < 0.05$ ($n = 3$, two-way ANOVA and Student's paired t test).

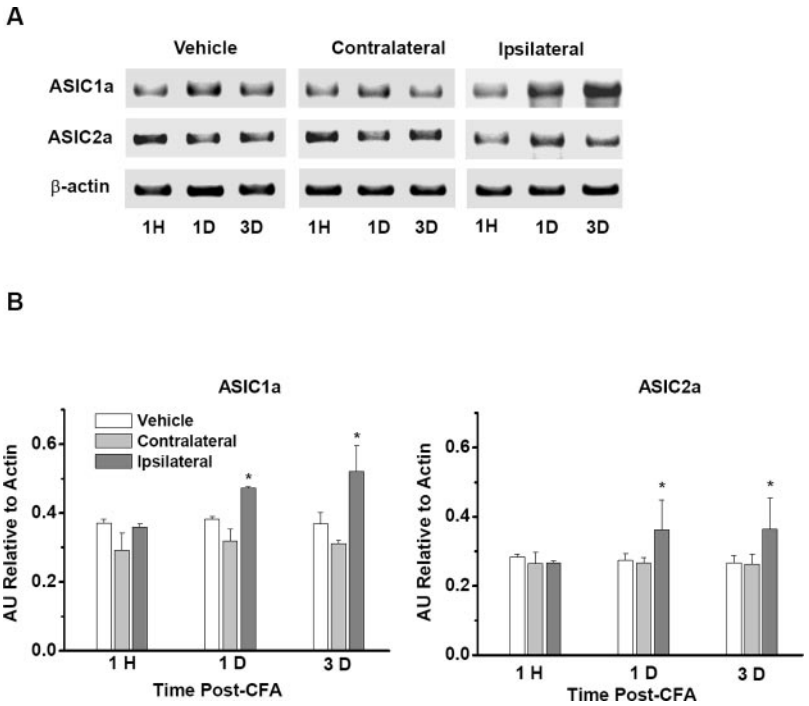

FIG. 7. **Up-regulation of dorsal horn ASIC1a and ASIC2a transcripts by periphery inflammation.** *A*, representative experiments showing RT-PCR products of ASIC1a and ASIC2a transcripts in L4–L5 spinal cord from vehicle and CFA-treated rats. *B*, ipsilateral spinal cord showed a significant increase in band intensity (normalized to β-actin) of ASIC1a and ASIC2a at day 1 and 3 compared with contralateral or vehicle control spinal cord. *, $p < 0.05$ ($n = 3$, two-way ANOVA and Student's paired t test).

atively higher Ca^{2+} permeability for ASIC1a than the other two channel combinations (39). Third, the heteromers of ASIC1a + 2a and ASIC2a + 2b show slow decaying kinetics, with the residual current still recorded at the end of the pH drop (9, 32, 35) but differing significantly from the present proton-gated currents. Fourth, the homomers of ASIC2a and

heteromers of ASIC1a + 2a are less sensitive to the inhibition of high $[Ca^{2+}]_o$ in transfected COS cells (33), and they can be potentiated by $[Zn^{2+}]_o$ (32). However, homomeric ASIC1a channels expressed in *Xenopus* oocyte could be inhibited by high $[Ca^{2+}]_o$ (7) but not by $[Zn^{2+}]_o$ (32), and similar results were observed for the proton-induced currents in the present preparation. Finally, the slow desensitization and the sustained current of the ASIC1a + 2a + 2b current exclude its involvement in native channel complex mediating the proton-induced current in spinal dorsal horn neurons. Interestingly, our results showed that ASIC1a + 2b had similar properties to those of homomeric ASIC1a, as well as native channels, suggesting the existence of functional ASIC1a + 2b channel complex (9, 40, 41). In conclusion, a reasonable explanation would be that homomeric ASIC1a and/or heteromeric ASIC1a + 2b channels mediate the proton-gated currents described herein. Electrophysiological analysis of hippocampal neurons from ASIC1 knock-out mice have identified a strict requirement for ASIC1a for proton-gated current in hippocampus (20). The expression of homomeric ASIC1a was also suggested in cerebellar granule cells (42).

Although our data show that an ASIC-like current appears to be the main ASIC current of spinal dorsal horn neurons, we could not completely excluded the possible involvement of ASIC2a and ASIC2b for the following reasons. First, ASIC2a and ASIC2b isoforms were detected in spinal dorsal horn neurons. Second, the slowly decaying ASIC current was expressed in a minority of recorded neurons (19/200). Third, some published data have suggested the existence of functional ASIC1a + 2a in central neurons (31, 43). Finally, one would expect even more complexity of native ASIC channels given that the intersubunit regulation of ASICs has been reported. For example, ASIC2a affects the kinetics of ASIC1a (35, 40), whereas ASIC2b reduces ASIC2a-mediated current (40). Nevertheless, the present results suggest that ASIC1a is the predominant ASIC subtype expressed in the majority of spinal dorsal horn neurons.

Functional Implications in Spinal Synaptic Function—Repetitive stimulation of the dorsal root evoked transient acidification in the dorsal horn by 0.25 pH units (44). The localized changes in synaptic cleft might be more pronounced because of the limited spatial and temporal resolution of pH microelectrodes in the measurement (37). Thus, ASICs of dorsal horn neurons might detect acidification associated with synaptic activity (20, 44).

A previous study has suggested an interaction between ASIC1a and NMDA receptors in the processing of learning and memory in hippocampal neurons (20). Interestingly, the development of spinal hyperexcitability and persistent pain also involves activation of NMDA receptors (45). Because there is a dramatic increase in primary afferent input after persistent noxious stimulation, synaptic activation of spinal NMDA receptors is also increased (46). We hypothesized that ASIC-like currents play an important role in spinal synaptic function under physiological and/or pathological conditions. In support of this hypothesis, we showed that activation of ASIC-like currents increased membrane depolarization of spinal dorsal horn neurons in an extracellular pH-dependent manner, which is expected to be sufficient to facilitate the release of NMDA receptor Mg^{2+} block.

Physiological/Pathological Significance—Our results provide strong evidence that ASICs serve as an important role in spinal second order sensory neurons. Injury that often causes persistent pain increases ASIC1a expression in periphery nociceptors (23) and may increase DRG neuron excitability (24). It is well known that increases in neuronal activity in response to inflammation lead to changes in gene expression in both peripheral and central nervous system, which appears to contribute to the hyperalgesia and allodynia in persistent pain (47, 48). It is, therefore, conceivable that the up-regulation of ASICs may be due to the activity-dependent expression during inflammation. Indeed, it has been demonstrated that the transcriptional activity of the ASIC3-encoding gene in DRG was enhanced by the proinflammatory mediators, such as nerve growth factor and serotonin (24). Interestingly, our results showed that periphery inflammation increased both ASIC1a and ASIC2a (but not ASIC2b) expression in spinal dorsal horn. As ASIC2a and ASIC2b are the splice variants, the different changes in expression of the two subunits may result from the regulation of splice site choices. Although further experiments are needed to elucidate the detailed mechanisms for this difference, we have found that the increased ASICs would lead to excitatory effects on the synaptic activity and hyperexcitability of spinal dorsal horn neurons, which may be related to behavioral hyperalgesia and allodynia. Accordingly, inflammatory pain could be the consequence of a combination of transcriptional changes in nociceptors and in dorsal horn neurons (47, 48). Future experiments with ASIC gene knock-out mice (20) and the selective ASIC receptor antagonist (42) will provide more insight into the roles of ASICs in spinal synaptic physiology and central pain sensation.

Acknowledgments—We thank Drs. Zhi-Qi Zhao and Yu-Qiu Zhang for helpful discussions, Wen Zhang, Yu Ding, Jr., Wei Wang, and Ru-Jia Sun for technical assistance, and Dr. Shanelle Ko for critical reading.

REFERENCES

1. Reeh, P. W., and Steen, K. H. (1996) *Prog. Brain Res.* **113,** 143–151
2. Caterina, M. J., Leffler, A., Malmberg, A. B., Martin, W. J., Trafton, J., Petersen-Zeitz, K. R., Koltzenburg, M., Basbaum, A. I., and Julius, D. (2000) *Science* **288,** 306–313
3. Waldmann, R., and Lazdunski, M. (1998) *Curr. Opin. Neurobiol.* **8,** 418–424
4. Reeh, P. W., and Kress, M. (2001) *Curr. Opin. Pharmacol.* **1,** 45–51
5. Price, M. P., Snyder, P. M., and Welsh, M. J. (1996) *J. Biol. Chem.* **271,** 7879–7882
6. Waldmann, R., Champigny, G., Voilley, N., Lauritzen, I., and Lazdunski, M. (1996) *J. Biol. Chem.* **271,** 10433–10436
7. Waldmann, R., Champigny, G., Bassilana, F., Heurteaux, C., and Lazdunski, M. (1997) *Nature* **386,** 173–177
8. Waldmann, R., Bassilana, F., de Weille, J., Champigny, G., Heurteaux, C., and Lazdunski, M. (1997) *J. Biol. Chem.* **272,** 20975–20978
9. Lingueglia, E., de Weille, J. R., Bassilana, F., Heurteaux, C., Sakai, H., Waldmann, R., and Lazdunski, M. (1997) *J. Biol. Chem.* **272,** 29778–29783
10. Chen, C. C., England, S., Akopian, A. N., and Wood, J. N. (1998) *Proc. Natl. Acad. Sci. U. S. A.* **95,** 10240–10245
11. Grunder, S., Geissler, H. S., Bassler, E. L., and Ruppersberg, J. P. (2000) *Neuroreport* **11,** 1607–1611
12. Akopian, A. N., Chen, C. C., Ding, Y., Cesare, P., and Wood, J. N. (2000) *Neuroreport* **11,** 2217–2222
13. Price, M. P., Lewin, G. R., McIlwrath, S. L., Cheng, C., Xie, J., Heppenstall, P. A., Stucky, C. L., Mannsfeldt, A. G., Brennan, T. J., Drummond, H. A., Qiao, J., Benson, C. J., Tarr, D. E., Hrstka, R. F., Yang, B., Williamson, R. A., and Welsh, M. J. (2000) *Nature* **407,** 1007–1011
14. Price, M. P., McIlwrath, S. L., Xie, J., Cheng, C., Qiao, J., Tarr, D. E., Sluka, K. A., Brennan, T. J., Lewin, G. R., and Welsh, M. J. (2001) *Neuron* **32,** 1071–1083
15. Lin, W., Ogura, T., and Kinnamon, S. C. (2002) *J. Neurophysiol.* **88,** 133–141
16. Ugawa, S., Yamamoto, T., Ueda, T., Ishida, Y., Inagaki, A., Nishigaki, M., and Shimada, S. (2003) *J. Neurosci.* **23,** 3616–3622
17. Chen, C. C., Zimmer, A., Sun, W. H., Hall, J., and Brownstein, M. J. (2002) *Proc. Natl. Acad. Sci. U. S. A.* **99,** 8992–8997
18. Biagini, G., Babinski, K., Avoli, M., Marcinkiewicz, M., and Seguela, P. (2001) *Neurobiol. Dis.* **8,** 45–58
19. Johnson, M. B., Jin, K., Minami, M., Chen, D., and Simon, R. P. (2001) *J. Cereb. Blood Flow Metab.* **21,** 734–740
20. Wemmie, J. A., Chen, J., Askwith, C. C., Hruska-Hageman, A. M., Price, M. P., Nolan, B. C., Yoder, P. G., Lamani, E., Hoshi, T., Freeman, J. H., Jr., and Welsh, M. J. (2002) *Neuron* **34,** 463–477
21. Wemmie, J. A., Askwith, C. C., Lamani, E., Cassell, M. D., Freeman, J. H., Jr., and Welsh, M. J. (2003) *J. Neurosci.* **23,** 5496–5502
22. Ettaiche, M., Guy, N., Hofman, P., Lazdunski, M., and Waldmann, R. (2004) *J. Neurosci.* **24,** 1005–1012
23. Voilley, N., de Weille, J., Mamet, J., and Lazdunski, M. (2001) *J. Neurosci.* **21,** 8026–8033
24. Mamet, J., Baron, A., Lazdunski, M., and Voilley, N. (2002) *J. Neurosci.* **22,** 10662–10670
25. Scholz, J., and Woolf, C. J. (2002) *Nat. Neurosci.* **5,** (suppl.), 1062–1067

26. Alvarez de la Rosa, D., Krueger, S. R., Kolar, A., Shao, D., Fitzsimonds, R. M., and Canessa, C. M. (2003) *J. Physiol.* (*Lond.*) **546,** 77–87
27. Li, Y. X., Schaffner, A. E., Li, H. R., Nelson, R., and Barker, J. L. (1997) *Brain. Res. Dev. Brain Res.* **102,** 261–266
28. Li, Y. F., Wu, L. J., Li, Y., Xu, L., and Xu, T. L. (2003) *J. Physiol.* (*Lond.*) **552,** 73–87
29. Wu, L. J., Lu, Y., and Xu, T. L. (2001) *J. Neurosci. Methods* **108,** 199–206
30. Akaike, N., Krishtal, O. A., and Maruyama, T. (1990) *J. Neurophysiol.* **63,** 805–813
31. Baron, A., Waldmann, R., and Lazdunski, M. (2002) *J. Physiol.* (*Lond.*) **539,** 485–494
32. Baron, A., Schaefer, L., Lingueglia, E., Champigny, G., and Lazdunski, M. (2001) *J. Biol. Chem.* **276,** 35361–35367
33. de Weille, J., and Bassilana, F. (2001) *Brain Res.* **900,** 277–281
34. Immke, D. C., and McCleskey, E. W. (2003) *Neuron* **37,** 75–84
35. Bassilana, F., Champigny, G., Waldmann, R., de Weille, J. R., Heurteaux, C., and Lazdunski, M. (1997) *J. Biol. Chem.* **272,** 28819–28822
36. Champigny, G., Voilley, N., Waldmann, R., and Lazdunski, M. (1998) *J. Biol. Chem.* **273,** 15418–15422
37. Miesenbock, G., De Angelis, D. A., and Rothman, J. E. (1998) *Nature* **394,** 192–195
38. Dubner, R., and Ruda, M. A. (1992) *Trends Neurosci.* **15,** 96–103
39. Yermolaieva, O., Leonard, A. S., Schnizler, M. K., Abboud, F. M., and Welsh, M. J. (2004) *Proc. Natl. Acad. Sci. U. S. A.* **101,** 6752–6757
40. Askwith, C. C., Wemmie, J. A., Price, M. P., Rokhlina, T., and Welsh, M. J. (2004) *J. Biol. Chem.* **279,** 18296–18305
41. Hesselager, M., Timmermann, D. B., and Ahring, P. K. (2004) *J. Biol. Chem.* **279,** 11006–11015
42. Escoubas, P., De Weille, J. R., Lecoq, A., Diochot, S., Waldmann, R., Champigny, G., Moinier, D., Menez, A., and Lazdunski, M. (2000) *J. Biol. Chem.* **275,** 25116–25121
43. Varming, T. (1999) *Neuropharmacology* **38,** 1875–1881
44. Chvatal, A., Jendelova, P., Kriz, N., and Sykova, E. (1988) *Physiol. Bohemoslov.* **37,** 203–212
45. Woolf, C. J., and Thompson, S. W. (1991) *Pain* **44,** 293–299
46. Randic, M., Jiang, M. C., and Cerne, R. (1993) *J. Neurosci.* **13,** 5228–5241
47. Woolf, C. J., and Costigan, M. (1999) *Proc. Natl. Acad. Sci. U. S. A.* **96,** 7723–7730
48. Zhuo, M. (2002) *Drug Discov. Today* **7,** 259–267